ORIGINAL RESEARCH

Cerebral aneurysm wall thickness analysis using intraoperative microscopy: effect of size and gender on thin translucent regions

Laith M Kadasi,[1,2] Walter C Dent,[1] Adel M Malek[1,2]

[1]Cerebrovascular and Endovascular Division, Department of Neurosurgery, Tufts Medical Center, Boston, Massachusetts, USA
[2]Tufts University School of Medicine, Boston, Massachusetts, USA

Correspondence to
Dr A M Malek, Department of Neurosurgery, Tufts Medical Center, 800 Washington St, No 178, Boston, MA 02111, USA; amalek@tuftsmedicalcenter.org

Received 21 January 2012
Accepted 13 February 2012
Published Online First 3 March 2012

ABSTRACT

Objective Wall thickness is a poorly documented characteristic of cerebral aneurysms which may provide insight into adaptive aneurysmal growth, aneurysm rupture risk and response to endovascular treatment. The distribution of aneurysm wall thickness, as observed by intraoperative video microscopy, is described.

Methods 54 unruptured saccular cerebral aneurysms were selected based on the availability of intraoperative video obtained from patients undergoing microsurgical clipping. Aneurysms were assessed for the distribution of wall thickness based on color translucence and quantitation of pixel values at superthin translucent, intermediate and thick regions of the dome. The data were analyzed with respect to aneurysm morphology, location and associated demographic factors.

Results The mean proportions of tissue characteristic among all domes analyzed were found to be 27% superthin, 65% intermediate, and 8% thick. Smaller aneurysms having a maximal dimension D_{max} <7 mm had a higher proportion of superthin tissue (p=0.003) and lower thick tissue (p=0.001) content. Female gender was associated with a significantly higher proportion of superthin tissue at the aneurysm dome (p=0.038), with no statistical dependence seen with patient age, smoking status or anatomical location.

Conclusion The dome of unruptured aneurysms is a highly heterogeneous region with areas of variable thickness that appear to be intimately related to the process of aneurysm development. This inconstant property affects wall tensile stress, may play a role in aneurysm pathogenesis and focal rupture, and should be incorporated into future analyses of aneurysm rupture risk and mechanics.

INTRODUCTION

Aneurysm dome wall thickness is a poorly documented feature in the study of aneurysm pathogenesis and the clinical assessment of rupture risk. Histological assessment has shown that the aneurysm wall undergoes a dynamic process of destructive remodeling and dysregulation, featuring de-cellularization and apoptosis, collagen reorganization, degeneration of the internal elastic lamina and elastin fragmentation, de-endothelialization, thrombus formation and inflammatory infiltration.[1–5] Some aspects of this process may be focal in nature as a result of the local release of inflammatory destructive enzymes and endothelium derived factors, such as nitric oxide and prostaglandin I_2.[4 6–8] The ultimate consequence is a heterogeneous tissue distribution observable on surgical exploration of thick, intermediate and thin translucent regions of the aneurysm wall.[9–11] Many observed aneurysms possess clearly defined loci of translucency suggestive of focal weakness, potentially influencing local material stiffness and yield stress, predisposing these regions to rupture.[12] Wall thickness is highly variable between and within aneurysms and has been reported as ranging from 16 to 400 μm, with the majority between 30 and 200 μm.[5 8 13 14] Several studies have attempted to describe a continuum through which different stages of the aneurysm ageing process can be observed and identified based on aneurysm size, level of calcification and intraoperative appearance.[10 11 15] These attempts to describe intraoperative findings of the aneurysm wall thickness have resorted to categorical description (such as entirely thick, thin or a mixture) and have lacked quantitative analysis. In addition, aneurysm wall thickness may play an important role in the process of aneurysm regrowth or coil compaction that is often observed following coil embolization of certain lesions.

There is currently no established non-invasive in vivo approach to wall thickness measurement; properties of the vessel and aneurysm wall are not easily extracted from the image data used in many aneurysm visualization protocols. While advances in computational analysis are approaching the level of accurately mapping a heterogeneous wall thickness distribution,[16] current imaging modalities possess insufficient spatial resolution to estimate local differences in aneurysm wall tissue characteristics.[17] Recent approaches in the study on aneurysm risk assessment focus on size and morphology with a lack of integrated information on the relative distribution of wall degeneration across aneurysm types.[18–20] Other investigations model the hemodynamic stress distribution under the assumption of a homogeneous aneurysm wall of uniform thickness or as a rigid wall, ignoring any of the tensile stresses in the dome tissue that lead to rupture and consequent subarachnoid hemorrhage.

Unruptured aneurysms are highly variable in their size, compliance, integrity and susceptibility of rupture, and likely represent multiple stages of a progressive adaptation to focal weakness that may become interrupted in the event of rupture. In order to better understand the process resulting in a focal area of weakness degenerating to the point

J NeuroIntervent Surg: first published as 10.1136/neurintsurg-2012-010285 on 3 March 2012. Downloaded from http://jnis.bmj.com/ on November 15, 2026 at Tufts University Libraries. Protected by copyright, including for uses related to text and data mining, AI training, and similar technologies.

of rupture, we sought to quantitatively examine aneurysm domes using intraoperative microscopy imaging obtained during microsurgical clipping procedures, in order to analyze these with respect to aneurysm size, location and demographic factors to provide a better understanding of aneurysm dome properties.

PATIENTS AND METHODS

Patient selection

Fifty-four unruptured saccular cerebral aneurysms were selected based on availability of high resolution intraoperative microscopy obtained from patients undergoing microsurgical clipping of an intracranial aneurysm at our institution between November 2006 and May 2011. Aneurysms that were fusiform, partially dissected, or obscured by clotted blood were excluded from the analysis. Ruptured aneurysms were excluded from the study because of obscuration by blood and the more limited dome visualization noted in these cases. Similarly, ruptured aneurysms were not included in this study because of obscuration by blood and the more limited dome visualization noted in these cases. The study was performed under approval by the institutional review board (IRB No 9035).

Intraoperative video

All intraoperative images were captured through a Leica M525 OH4 surgical microscope video attachment with a Sony 3 chip CCD color digital video camera at 640×480 resolution during aneurysm clipping procedures (Leica Microsystems; Wetzlar, Germany; Sony, Tokyo, Japan). For all surgeries, the microscope magnification was approximately 10–12.8× with a working distance from microscope objective to aneurysm body of around 207–240mm. The video signal was recorded using the Leica MDRS4 (Medical Digital Recording System), encoding the digital signal as mpeg4 format at 5.1 Mbps. Representative intraoperative photographs of the aneurysm dome were extracted from the video data prior to pixel based analysis (figure 1A–D). Special care was taken to evaluate multiple projections of the target aneurysm to avoid the focal microscope light reflection artifact off of the dome (eg, figure 1A) as well as desiccated portions of the dome that had not been recently irrigated.

Semiquantitative wall thickness assessment

Intraoperative microscopy intraoperative video acquisitions were analyzed using GNU Image Manipulation Program (GIMP 2.6.8, Free Software Foundation, Boston, Massachusetts, USA). The available field of each aneurysm image, ranging from 30% to 90% of the entire aneurysm dome, was categorically segmented into red, superthin translucent portions and white or yellow thick calcified portions compared with healthy portions of the parent vessel. Data describing the thickness distribution of each aneurysm were obtained using semiautomated pixel thresholding (figure 2A–D) guided by manual area selection, with the remaining tissue matching the appearance of the healthy non-calcific proximal parent vessel being categorized as intermediate thickness. All comparisons among statistical groups were performed with JMP V.8.02 (SAS).

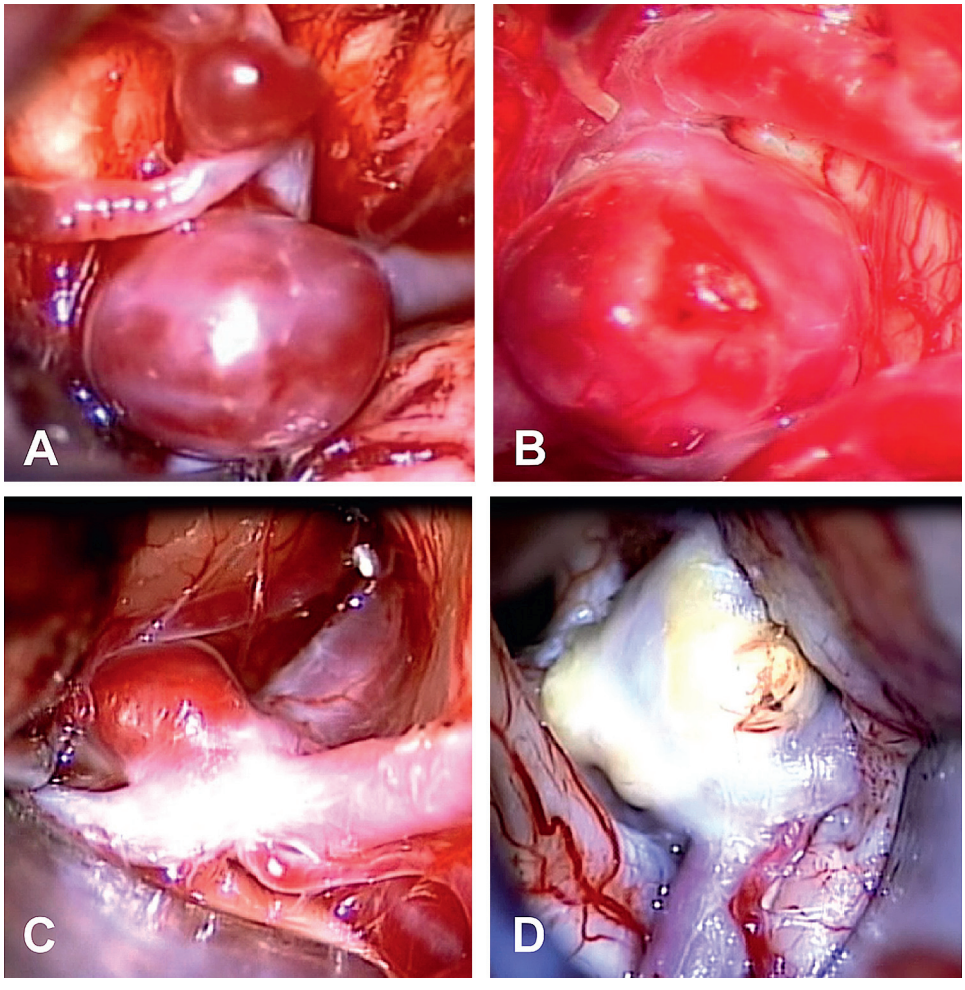


Figure 1 Intraoperative microscopic image of unruptured saccular aneurysms. (A) Middle cerebral artery aneurysm with a distribution of superthin (22%) and intermediate tissue (77%) (bottom) in contrast with a smaller inferior M2 division aneurysm composed almost entirely of superthin tissue (86%) (top). (B) Middle cerebral aneurysm with regions of superthin (49%), intermediate (48%) and thick regions (3%). (C) Anterior communicating artery aneurysm composed almost entirely of superthin tissue (82%). (D) Anterior communicating artery aneurysm with a large proportion of thick tissue (68%).

J NeuroIntervent Surg: first published as 10.1136/neurintsurg-2012-010285 on 3 March 2012. Downloaded from http://jnis.bmj.com/ on November 15, 2026 at Tufts University Libraries. Protected by copyright, including for uses related to text and data mining, AI training, and similar technologies.

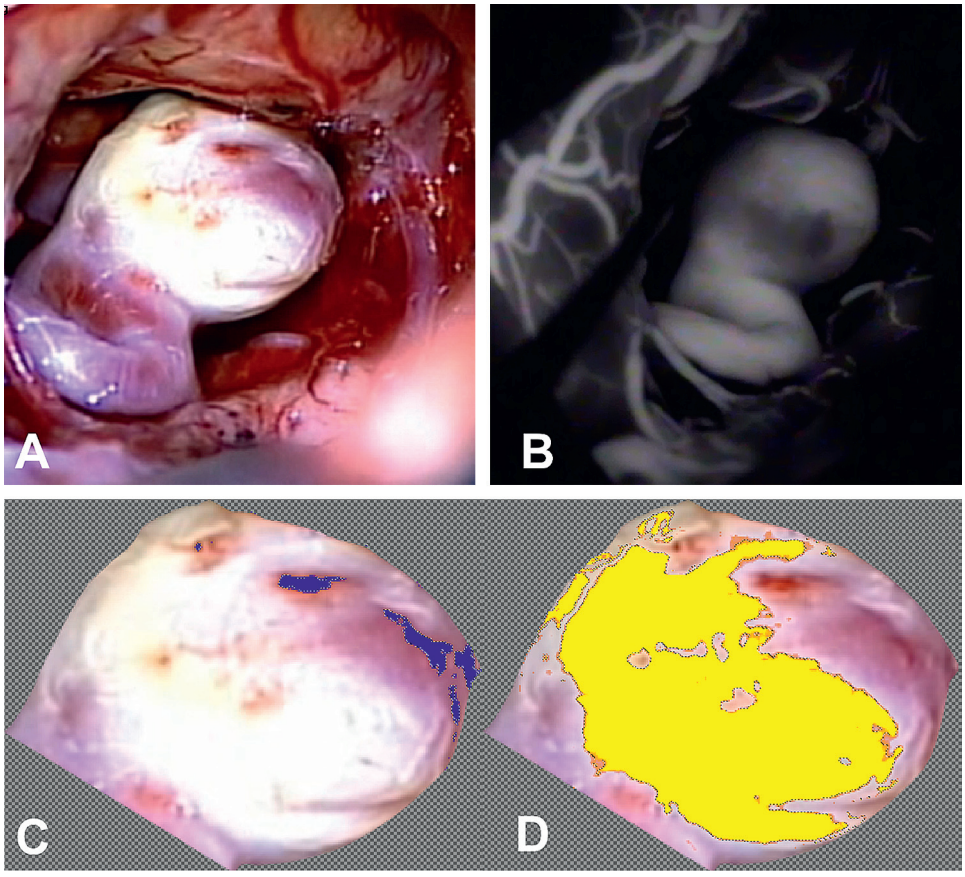


Figure 2 Intraoperative light microscopy (A) and corresponding fluorescein isothiocyanate fluorescence microscopy (B) of a middle cerebral artery aneurysm assessed via semiautomated color selection. Superthin regions (C, shown in blue) and thick regions (D, yellow) are recorded as per cent of total visible aneurysm dome tissue.

RESULTS

The study group consisted of 31 women and 16 men with a mean age of 54.1 (range 27–76 years) (table 1). The wall thickness distribution of 54 unruptured saccular aneurysms from 47 patients were analyzed with respect to age, gender, smoking status, maximal dimension, neck area and location. The distribution of the proportion of each dome thickness subset is shown for all aneurysms in figure 3. Importantly, 74.0% (n=40) of all aneurysms in the study group lacked any thick wall regions. The mean percentage of superthin, intermediate and thick tissue among all aneurysms was 27.0%, 64.9% and 8.1%, respectively (figure 4).

Patients with a prior or current history of smoking showed no statistically significant difference in the portion of aneurysm regions consisting of superthin (p=0.657) or thick tissue (p=0.969, table 2). Patient age (superthin, p=0.256; thick, p=0.192) and aneurysm location also showed no significant association with wall thickness distribution.

Analysis of aneurysm size using dome maximal dimension (D_{max}) revealed that aneurysms larger than 7 mm (n=12) had a smaller proportion of superthin translucent tissue compared with smaller lesions (p=0.003), and a larger proportion of thick calcified tissue regions (p=0.001). In addition, the proportion of superthin translucent tissue was significantly greater (p=0.038) in women compared with men, with no difference found in the ratio of thick tissue with gender (p=0.462).

Table 1 Demographic information

Aneurysm characteristics	No of cases (%)
Mean age (years)	54.1±12.43
Gender	
Men	16 (34.0)
Women	31 (65.9)
Aneurysm location	
Anterior cerebral	6 (11.1)
Anterior communicating artery	15 (27.8)
Internal carotid artery	4 (7.4)
Middle cerebral artery	26 (48.1)
Posterior communicating artery	3 (5.6)

DISCUSSION

This is the first study of its kind to analytically describe the distribution of aneurysm wall thickness through in vivo examination of the aneurysm dome. Semiquantitative analysis revealed wall thickness distribution to correlate with both patient gender and aneurysm size. Prior intraoperative and autopsy based observational studies have described the distribution using a simplified classification scheme based on categorical grouping of thick or thin with respect to the parent vessel wall.[10 11 15] Although these methods were useful in revealing a new potential path of study, the simplified dichotomous scheme of observation limited the potential accuracy of these studies and may explain the absence of any previous findings describing gender differences. Other approaches of aneurysm pathogenesis research which target rupture risk analysis and stratification typically exclude the assessment of aneurysm wall thickness information due to difficulty in imaging.[9 20–24] In spite of this omission, wall composition and thickness would appear to be among the most important candidates for analytical characterization given that the very mechanism of rupture results from a breach in the aneurysm wall.

Gender differences

A critical finding in this analysis is that of the relationship between patient gender and the distribution of wall thickness at

J NeuroIntervent Surg: first published as 10.1136/neurintsurg-2012-010285 on 3 March 2012. Downloaded from http://jnis.bmj.com/ on November 15, 2026 at Tufts University Libraries. Protected by copyright, including for uses related to text and data mining, AI training, and similar technologies.

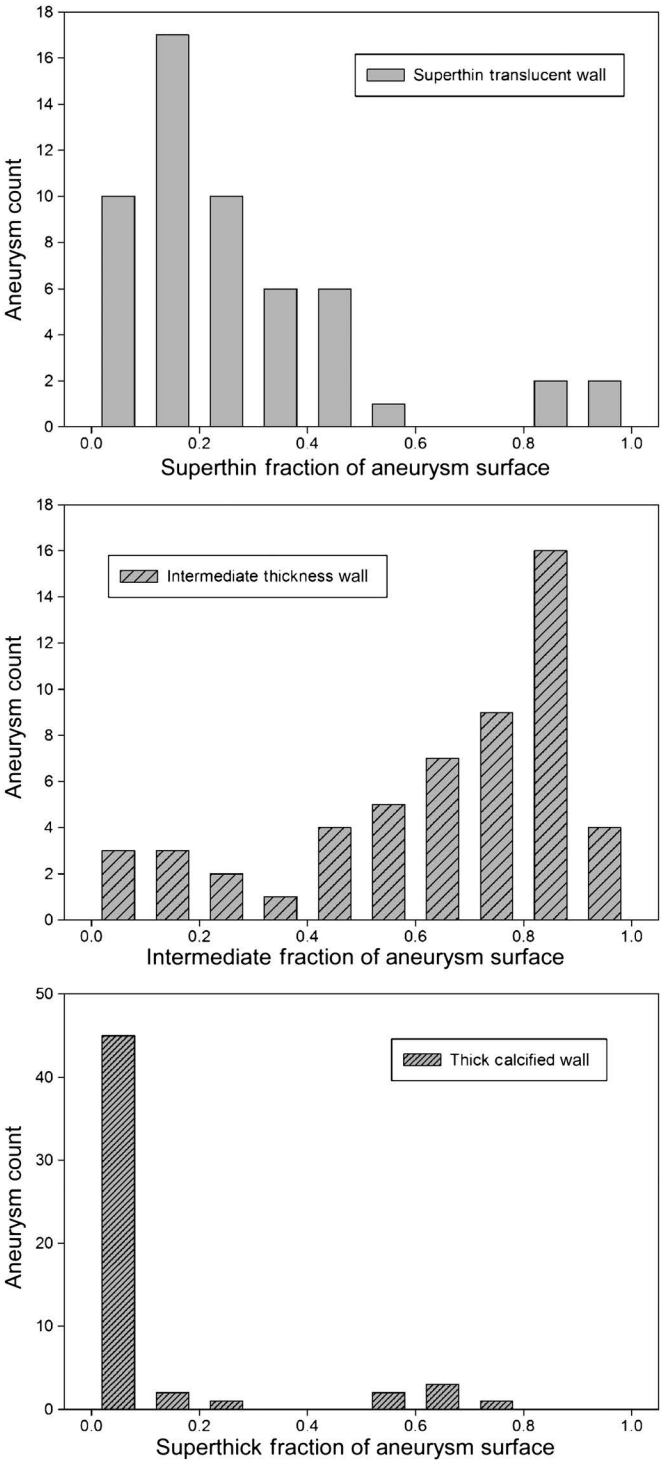


Figure 3 Histogram showing the distribution of superthin, intermediate and thick tissue fractions across all aneurysms.

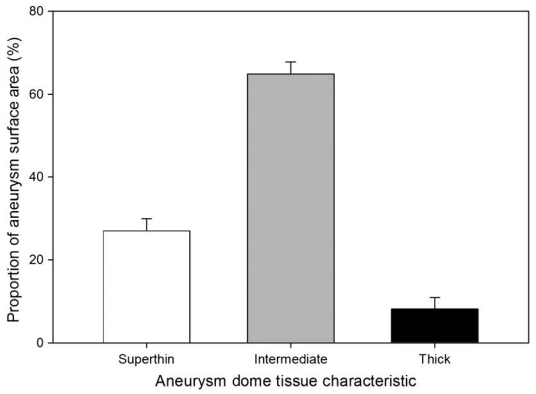


Figure 4 Mean distribution of dome wall thickness across all aneurysms.

the aneurysm dome in unruptured saccular aneurysms. Previous analyses of sex differences in the anterior circulation have illustrated that smaller vessel size and higher flow velocity contribute to increased subarachnoid hemorrhage rates in women.[15 24 25] The current findings indicate that these characteristics may parallel observable changes to the aneurysm wall, reflected by a greater proportion of superthin translucent tissue at the aneurysm dome among women. Interestingly, the difference in thick tissue across gender groups was not statistically significant. This raises questions as to whether aneurysms with a higher proportion of superthin translucent tissue or thick tissue may in fact be more susceptible to rupture.

Effect of aneurysm size

Another critical finding in this analysis is that aneurysms larger than 7 mm possess a significantly smaller proportion of superthin translucent tissue and a larger proportion of thick tissue. This finding further explores a size–pathogenesis relationship originally described in a study by Asari and Ohmoto in 1994, documenting a subset of entirely thick walled aneurysms, all of which were found to be greater than 9 mm in maximal dimension,[10] and reaffirmed by Mizoi and *et al* in 1996 with the finding that entirely thick walled aneurysms were significantly larger in mean size than entirely thin walled aneurysms.[11] Although smaller aneurysms are traditionally considered to possess a lower risk of aneurysm rupture,[18] small aneurysms with greater regions of superthin translucent tissue may in fact grow at an increased rate, further confounding the use of size as a determinant of risk. Based on the evidence presented by studies using direct aneurysmal observation, large cerebral aneurysms possessing thick or calcified tissue may represent an advanced stage in the ageing process of aneurysms that successfully avoid rupture.[10 11 15] Histological analyses have also identified thick intima-like aneurysm walls as more frequent in younger patients and less prone to rupture than thin hyalinized walls.[1–5] Exploration of the relationship between patient age, wall adaptive

Table 2 Aneurysm wall thickness distribution

Characteristic	Superthin tissue proportion (%)	p Value	Thick calcified tissue proportion (%)	p Value
Patient age		0.256		0.192
Age >45 years	28.6±3.3		9.8±3.0	
Age <45 years	19.9±6.9		0.6±6.3	
Aneurysm maximal dimension		0.003*		0.001*
D_{max} >7 mm	12.2±5.9		22.0±4.8	
D_{max} <7 mm	33.4±3.4		2.6±2.7	
Patient gender		0.038*		0.462
Men	17.5±5.3		11.2±5.0	
Women	31.0±3.4		6.8±3.3	
Smoking status		0.657		0.969
Non-smoker	24.5±12.1		9.4±5.2	
Current smoker	30.4±29.1		7.7±4.8	
Prior smoker	24.2±22.0		8.9±5.2	

*Significant difference.

J NeuroIntervent Surg: first published as 10.1136/neurintsurg-2012-010285 on 3 March 2012. Downloaded from http://jnis.bmj.com/ on November 15, 2026 at Tufts University Libraries. Protected by copyright, including for uses related to text and data mining, AI training, and similar technologies.

maintenance mechanisms and vessel calcification may be beneficial in future studies.

Implications of heterogeneous wall thickness to endovascular therapy response

Aneurysm wall calcification is a critical characteristic that affects the ability to provide secure surgical clipping and can necessitate alternate clip reconstruction techniques to successfully isolate the dome. On the other hand, one can hypothesize that some of the limitations with current aneurysm endovascular therapy, such as coil compaction or aneurysm regrowth, may stem from heterogeneous aneurysm wall thickness. The high risk of recurrence following coiling (~21%) and the risk of major recurrence necessitating retreatment[26] could be the result of preferential coil compaction into thinner aneurysm wall regions. Clipping of recanalized previously coiled aneurysms often reveals extravasation of the coil mass into the surrounding subarachnoid space,[27 28] a phenomenon usually attributed to the presence of intraluminal thrombus. Our findings suggest an alternate hypothesis in which coils preferentially protrude through the thinner translucent wall regions compared with the thicker stiffer regions. Further exploration of the distribution of superthin translucent and thick calcified regions of the aneurysm wall and understanding differences in the physical properties between these regions could help understand any links with failure rates of coil based endovascular therapy and devise improved therapeutic strategies.

Study limitations

As noted in the methods section, intraoperative microscopy did not allow circumferential visualization of the entire aneurysm dome in all cases, and was restricted to a mean of 63% of the total surface area of the aneurysm dome and neck. It also must be noted that the semiquantitative assessment of wall thickness based on visual appearance provides no quantitative detail of exact tissue thickness and represents an approximation. In addition, although recognized and compensated for during the acquisition process, one cannot avoid the small contribution of the local differences in tissue hydration and light source reflection.

Although it is implied that the translucent superthin regions of the aneurysm dome would be more likely to be prone to rupture, this may not be necessarily the case, and it is possible that any rupture and subsequent subarachnoid hemorrhage would occur elsewhere at the aneurysm dome. This study was limited to unruptured saccular aneurysms in the anterior circulation, and the associations found may not apply to ruptured cerebral aneurysms or aneurysms of the posterior circulation. On the other hand, to avoid the inaccuracies inherent as a result of the presence of coagulated blood that is not manually excluded by the surgeon, the study was limited to unruptured aneurysms.

Future directions

Intraoperative microscopy could be beneficially integrated with other methods of rupture risk assessment, such as computational fluid dynamic techniques, to more accurately determine the hemodynamic stress distribution at the aneurysm wall and correlate the latter with wall properties. Similarly, fluid–structure interaction quantitative analysis that incorporates not only wall thickness but a heterogeneous tissue distribution coupled with fluid dynamics would allow for increased model accuracy. Ultimately, the ability to extract detailed tissue distribution information from non-invasive medical imaging may contribute greatly to the improved assessment of aneurysm rupture risk.

Several approaches are worthy of consideration in the future of aneurysm wall thickness assessment although they are each associated with obstacles that must be addressed in turn. Intravascular ultrasound may serve as a potential approach but is associated with high cost as well as an attendant risk of dissection, thromboembolism or aneurysm rupture, not to mention its ethical use in the absence of demonstrated predictive potential. Electrocardiographically gated CT angiography has also been applied to detect pulsation at the aneurysm wall as an approximation of the thinnest regions of the aneurysm dome[29] but requires further exploration in order to validate method accuracy. It is worth noting that studies applying this method have noted pulsation of the aneurysm wall at the thinnest regions of the aneurysm dome, which were not observed in any of the intraoperative video analyses performed in the current study, albeit in unruptured aneurysms. Indirect measurement of wall thickness using the digital analysis of aneurysm bruit has also been considered with some experimental validation[30] but also requires further exploration before it can be applied clinically.

CONCLUSION

The aneurysm wall is a highly variable region containing areas of thick, intermediate and superthin translucent tissue, each of which are distinguishable and quantifiable via intraoperative observation. These differences vary systematically with aneurysm size and patient gender, and have been associated with aneurysm pathogenesis and rupture in both histological and intraoperative observational studies. Future exploration of beneficial and pathological adaptive remodeling mechanisms in cerebral aneurysms should incorporate direct observation of aneurysm dome wall properties.

Acknowledgments The authors thank Alexandra Lauric, PhD, for her assistance.

Contributors AMM: concept and study design; LMK and WCD: data acquisition; LMK and AMM: data analysis and manuscript preparation.

Competing interests None.

Ethics approval Ethics approval was provided by Tufts Institutional Review Board.

Provenance and peer review Not commissioned; externally peer reviewed.

REFERENCES

1. **Frosen J,** Piippo A, Paetau A, *et al*. Remodeling of saccular cerebral artery aneurysm wall is associated with rupture: histological analysis of 24 unruptured and 42 ruptured cases. *Stroke* 2004;**35**:2287–93.
2. **Meng H,** Wang Z, Hoi Y, *et al*. Complex hemodynamics at the apex of an arterial bifurcation induces vascular remodeling resembling cerebral aneurysm initiation. *Stroke* 2007;**38**:1924–31.
3. **Abruzzo T,** Shengelaia GG, Dawson RC 3rd, *et al*. Histologic and morphologic comparison of experimental aneurysms with human intracranial aneurysms. *AJNR Am J Neuroradiol* 1998;**19**:1309–14.
4. **Kondo S,** Hashimoto N, Kikuchi H, *et al*. Apoptosis of medial smooth muscle cells in the development of saccular cerebral aneurysms in rats. *Stroke* 1998;**29**:181–8.
5. **MacDonald DJ,** Finlay HM, Canham PB. Directional wall strength in saccular brain aneurysms from polarized light microscopy. *Ann Biomed Eng* 2000;**28**:533–42.
6. **Frangos JA,** Eskin SG, McIntire LV, *et al*. Flow effects on prostacyclin production by cultured human endothelial cells. *Science* 1985;**227**:1477–9.
7. **Rubanyi GM,** Romero JC, Vanhoutte PM. Flow-induced release of endothelium-derived relaxing factor. *Am J Physiol* 1986;**250**:H1145–9.
8. **Scott S,** Ferguson GG, Roach MR. Comparison of the elastic properties of human intracranial arteries and aneurysms. *Can J Physiol Pharmacol* 1972;**50**:328–32.
9. **Hassan T,** Timofeev EV, Saito T, *et al*. A proposed parent vessel geometry-based categorization of saccular intracranial aneurysms: computational flow dynamics analysis of the risk factors for lesion rupture. *J Neurosurg* 2005;**103**:662–80.
10. **Asari S,** Ohmoto T. Growth and rupture of unruptured cerebral aneurysms based on the intraoperative appearance. *Acta Med Okayama* 1994;**48**:257–62.
11. **Mizoi K,** Yoshimoto T, Nagamine Y. Types of unruptured cerebral aneurysms reviewed from operation video-recordings. *Acta Neurochir (Wien)* 1996;**138**:965–9.

J NeuroIntervent Surg: first published as 10.1136/neurintsurg-2012-010285 on 3 March 2012. Downloaded from http://jnis.bmj.com/ on November 15, 2026 at Tufts University Libraries . Protected by copyright, including for uses related to text and data mining, AI training, and similar technologies.

12. **Steiger HJ,** Aaslid R, Keller S, *et al*. Strength, elasticity and viscoelastic properties of cerebral aneurysms. *Heart Vessels* 1989;**5**:41—6.
13. **Isaksen JG,** Bazilevs Y, Kvamsdal T, *et al*. Determination of wall tension in cerebral artery aneurysms by numerical simulation. *Stroke* 2008;**39**:3172—8.
14. **Suzuki J,** Ohara H. Clinicopathological study of cerebral aneurysms. Origin, rupture, repair, and growth. *J Neurosurg* 1978;**48**:505—14.
15. **Inagawa T,** Hirano A. *Autopsy study of unruptured incidental intracranial aneurysms*. New York, NY: Elsevier, 1990.
16. **Xuefeng Z,** Madhavan LR, Jia L. Characterizing heterogeneous properties of cerebral aneurysms with unknown stress-free geometry: a precursor to in vivo identification. *J Biomech Eng* 2011;**133**:051008.
17. **Balocco S,** Camara O, Vivas E, *et al*. Feasibility of estimating regional mechanical properties of cerebral aneurysms in vivo. *Med Phys* 2010;**37**:1689—706.
18. **Wiebers DO,** Whisnant JP, Huston J 3rd, *et al*. Unruptured intracranial aneurysms: natural history, clinical outcome, and risks of surgical and endovascular treatment. *Lancet* 2003;**362**:103—10.
19. **Xiang J,** Natarajan SK, Tremmel M, *et al*. Hemodynamic-morphologic discriminants for intracranial aneurysm rupture. *Stroke* 2011;**42**:144—52.
20. **Baharoglu MI,** Schirmer CM, Hoit DA, *et al*. Aneurysm inflow-angle as a discriminant for rupture in sidewall cerebral aneurysms: morphometric and computational fluid dynamic analysis. *Stroke* 2010;**41**:1423—30.
21. **Shojima M,** Oshima M, Takagi K, *et al*. Magnitude and role of wall shear stress on cerebral aneurysm: computational fluid dynamic study of 20 middle cerebral artery aneurysms. *Stroke* 2004;**35**:2500—5.
22. **Boussel L,** Rayz V, McCulloch C, *et al*. Aneurysm growth occurs at region of low wall shear stress: patient-specific correlation of hemodynamics and growth in a longitudinal study. *Stroke* 2008;**39**:2997—3002.
23. **Cebral JR,** Mut F, Weir J, *et al*. Association of hemodynamic characteristics and cerebral aneurysm rupture. *AJNR Am J Neuroradiol* 2011;**32**:264—70.
24. **Lindekleiv HM,** Valen-Sendstad K, Morgan MK, *et al*. Sex differences in intracranial arterial bifurcations. *Gend Med* 2010;**7**:149—55.
25. **Eden SV,** Meurer WJ, Sanchez BN, *et al*. *Gender and ethnic differences in subarachnoid hemorrhage*. Hagerstown, MD: Lippincott Williams & Wilkins, 2008.
26. **Raymond J,** Guilbert F, Weill A, *et al*. Long-term angiographic recurrences after selective endovascular treatment of aneurysms with detachable coils. *Stroke* 2003;**34**:1398—403.
27. **Horowitz M,** Samson D, Purdy P. Does electrothrombosis occur immediately after embolization of an aneurysm with Guglielmi detachable coils? *AJNR Am J Neuroradiol* 1997;**18**:510—13.
28. **Doerfler A,** Wanke I, Egelhof T, *et al*. Aneurysmal rupture during embolization with Guglielmi detachable coils: causes, management, and outcome. *AJNR Am J Neuroradiol* 2001;**22**:1825—32.
29. **Hayakawa M,** Katada K, Anno H, *et al*. CT angiography with electrocardiographically gated reconstruction for visualizing pulsation of intracranial aneurysms: identification of aneurysmal protuberance presumably associated with wall thinning. *AJNR Am J Neuroradiol* 2005;**26**:1366—9.
30. **Jou LD,** Mawad ME. Indirect measurement of aneurysm wall thickness using digital stethoscope. *Neurol Res* 2010;**32**:661—5.

J NeuroIntervent Surg: first published as 10.1136/neurintsurg-2012-010285 on 3 March 2012. Downloaded from http://jnis.bmj.com/ on November 15, 2026 at Tufts University Libraries .
Protected by copyright, including for uses related to text and data mining, AI training, and similar technologies.